Accepted by the Astrophysical Journal

Nucleosynthesis and Mixing in Cassiopeia A

John P. Hughes[1,2], Cara E. Rakowski[1,2], David N. Burrows[3], and Patrick O. Slane[4]

ABSTRACT

We present results from the first light observations of the Cassiopeia A (Cas A) supernova remnant (SNR) by the *Chandra* X-ray Observatory. The X-ray spectrum varies on all spatial scales down to the instrumental limit (0.02 pc at the SNR). Based on representative spectra from four selected regions we investigate the processes of nucleosynthesis and mixing in Cas A. We make the first unequivocal identification of iron-rich ejecta produced by explosive silicon-burning in a young Galactic SNR. Elsewhere in the remnant we see silicon-rich ejecta from explosive oxygen-burning. Remarkably, our study finds that the Fe-rich ejecta lies outside the Si-rich material, leading to the conclusion that bulk motions of the ejecta were extensive and energetic enough in Cas A to cause a spatial inversion of a significant portion of the supernova core during the explosion. It is likely that this inversion was caused by "Fe"-rich ejecta emerging in plumes from the rising bubbles in the neutrino-driven convection layer. In addition the radioactive decay energy from ^{56}Ni may have contributed to the subsequent evolution of the material. We have also discovered faint, well-defined filaments with featureless X-ray spectra that are possibly the sites of cosmic ray acceleration in Cas A.

Subject headings: ISM: individual (Cassiopeia A) — nuclear reactions, nucleosynthesis, abundances — supernova remnants — X-rays: ISM

1. INTRODUCTION

Young supernova remnants (SNRs) are the critical link between the nucleosynthetic processes that occur in stars and essentially all the metals that exist in the Universe. Accurate knowledge

[1]Department of Physics and Astronomy, Rutgers The State University of New Jersey, 136 Frelinghuysen Road, Piscataway NJ 08854-8019; E-mail: jph@physics.rutgers.edu and rakowski@physics.rutgers.edu

[2]Also Service d'Astrophysique, L'Orme des Merisiers, CEA-Saclay, 91191 Gif-sur-Yvette Cedex France

[3]Department of Astronomy & Astrophysics, 525 Davey Lab, Penn State University, University Park, PA 16802

[4]Harvard-Smithsonian Center for Astrophysics, 60 Garden Street, Cambridge MA 02138

of the nucleosynthetic yields from exploded stars is essential for studies of the evolution of the interstellar medium, external galaxies, and even clusters of galaxies. However, models of nucleosynthesis have been tested almost exclusively in the ensemble (i.e., averaged over a stellar initial mass function) by comparison against meteoritic and solar photospheric abundances (e.g., Thielemann, Nomoto, & Hashimoto 1996, hereafter TNH). Direct comparison of the models against abundance data derived from individual supernovae (SNe) or their remnants has been much more limited (e.g., Hughes & Singh 1994).

Numerical models (e.g., Woosley & Weaver 1995; TNH) predict that nucleosynthesis in core-collapse SN occurs in a layered, "onion"-skin type manner. Near the core of the star where the burning shock temperatures are highest, explosive Si-burning completely exhausts Si and results in a composition that is dominated by ^{56}Ni, which, as it decays to ^{56}Co and ^{56}Fe, powers the light curve of the supernova. Further out from the center of the star the shock temperature has dropped and explosive Si-burning is incomplete. In this zone significant amounts of what will ultimately become Fe are still produced, but a large fraction of the matter is left in the form of Si, S, Ar, and Ca. At lower temperatures and further out still, explosive O-burning occurs, leading to a composition dominated by O and Si with very little or no Fe. Finally, there is explosive Ne/C-burning which produces mostly O. At this point, the temperature of the burning shock has fallen far enough that the composition of layers of the star above are unaltered by the SN explosion. Instead they reflect the nucleosynthesis that occurred during the normal course of the star's hydrostatic evolution.

The high sensitivity, broad bandwidth, good spectral resolution, and unsurpassed angular resolution of the recently launched *Chandra* X-ray Observatory (see Weisskopf et al. 1996 for a description) has opened up a new window on the explosive nucleosynthesis process in supernovae. It is now possible to measure the composition of individual knots within SNRs and, by comparison to models of the nucleosynthetic process, determine in what layer or layers of the progenitor star the material was formed. In this letter we report on early *Chandra* observations of the Cassiopeia A (Cas A) SNR in which we demonstrate for the first time this powerful new technique.

Cas A is widely believed to be the result of a core collapse supernova explosion of a massive star (Fesen et al. 1987) that was possibly witnessed by Flamsteed in 1680 and was rediscovered as a remnant in the radio by Ryle & Smith (1948) over 250 years later. At a distance of 3.4 kpc (Reed et al. 1995), the $2'$ radius optical shell corresponds to a physical size of 1.7 pc. In the optical band, Cas A displays complex variations of composition with position and velocity, and it is one of the brightest SNRs at X-ray and radio frequencies.

2. OBSERVATIONS AND DATA REDUCTION

Cas A was observed for 6,100 s by ACIS-S (Garmire 1997) on 20 August, 1999, during Orbital Activation and Check-out of *Chandra*. A processed event file of the observation (with creation

date 1999-09-04T03:08:28) was obtained from the *Chandra* X-ray Center and analysis was carried out using standard astronomical software. The spectra were extracted using the energy column from the *Chandra* event file and binned into energy channels containing at least 25 events each. At this point the calibration of the instrument is still preliminary; for example, the energy scale of the spectral data may be uncertain by tens of percent. Nevertheless the bright, well-known spectral features in the remnant's spectrum allow for the nearly unambiguous identification of emission from the astrophysically abundant elements Mg, Si, S, Ar, Ca, and Fe. For comparison to observed spectra we use preliminary response functions for the effective area of the telescope (acis_bi.arf) and the efficiency and spectral resolution of the ACIS-S instrument (w134c4r_norm.rmf) convolved with simple models for the X-ray emission from SNRs, including the effects of nonequilibrium, or time dependent, ionization (NEI) (Hughes & Singh 1994). In this letter we aim for a qualitative description of several representative *Chandra* spectra; quantitative studies with formal χ^2-type fits to the data are deferred to future work.

3. DATA ANALYSIS AND DISCUSSION

3.1. Image Analysis

A color image of Cas A, encoding information on the intrinsic X-ray spectrum of the remnant, is shown in Figure 1. Regions that appear red indicate places where Cas A shows more emission from the energy band (0.6–1.65 keV) that contains the K-shell lines (transitions to the 1s electronic level) of O, Ne, and Mg and L-shell lines (transitions to the 2s electronic level) of Ca and Fe. Green regions are relatively enhanced in the K-shell emission lines of Si (energy band 1.65–2.25 keV), while blue regions are weighted toward higher energy emission (2.25–7.50 keV) that includes the S, Ar, Ca, and Fe K-shell emission lines. Regions with comparable levels of emission in the three bands appear white. All three bands also contain emission from thermal bremsstrahlung as well as other nonthermal continuum components.

The overall, gross morphology of Cas A has been known from earlier studies, but the exquisitely fine spatial details of its X-ray emission apparent in Fig. 1 (and Fig. 2, the broadband total intensity X-ray image) are entirely without precedent. Furthermore, the *Chandra* data show that the X-ray spectral character of the SNR varies on all angular scales down to the resolution limit of the telescope ($\sim 1''$), which corresponds to physical scales of $\sim$0.02 pc at the remnant. Features of the X-ray remnant to note (colors refer to Fig. 1) are (1) the outer blast-wave, which fully surrounds the remnant and appears reddish-purple; (2) diffuse clumps of reddish emission most obvious to the east and north; (3) bright compact knots (largely green or white-colored) within the bright shell; and (4) diffuse filamentary emission pervading the interior, which varies considerably in color. As we illustrate below, using spectra from four representative regions, spectral differences arise from variations in the underlying radiation process, composition, excitation conditions, and the column density of absorbing gas and dust in the line-of-sight toward

Cas A.

3.2. Spectral Analysis of Stellar Ejecta

The compact, high surface brightness knots are among the most striking new features of the *Chandra* Cas A image. In Figure 3 we show the spectrum of one such feature, namely the bright green-colored knot toward the SE labeled A in Fig. 2. The dominant spectral feature is the (unresolved) complex of K-shell transitions from the helium-like ion of Si at a photon energy of ∼1.85 keV although the spectrum also contains emission from other elemental species: Mg, S, Ar and Ca. This knot displays the largest equivalent width Si line we have yet detected in the remnant, $W_E = 1.6\,\mathrm{keV}$, more than twice the maximum equivalent width expected from a hot plasma with solar abundances under NEI conditions, $W_E = 0.6\,\mathrm{keV}$. On the other hand, the equivalent width of the Si line is far smaller than the value expected from a knot of pure Si or even a knot of pure metal ejecta composed only of those elemental species with observed K-shell line emission. A number of other compact features in the remnant share these characteristics, although with slightly less dominant Si lines, including many of the white unresolved knots in the northern section of the bright shell.

The enhanced Si and S abundances, relative to solar, identify these compact knots as stellar ejecta from deep within the progenitor star where explosive O-burning or incomplete Si-burning took place (TNH). The elemental species with K-shell lines in the observed band are unable to produce sufficient continuum emission to explain the amount seen and so another source for the continuum is required. Additional material with low enough atomic number ($Z < 8$) that its emission lines fall below the observed band is required (a solar abundance plasma produces too much Fe L-shell emission). The spectral model plotted against the spectrum from region A as the solid line in Fig. 3 is a representation of this situation: it contains the products of explosive O-burning in the predicted ratios from TNH (taken from their Table 2) plus a H/He continuum (a N-rich plasma would work as well for the continuum). Parameters describing the thermodynamic state of the plasma (temperature, ionization timescale, and line-of-sight absorbing column density) were adjusted for broad agreement with the observed line shapes. All of the obvious line features in the spectrum from this region can be described by emission from species that are predicted to be produced in explosive O-burning. In particular we note the low energy features from Ca L-shell lines (0.65 keV and 0.85 keV) and Mg K-shell emission (1.34 keV). Both of these species are observed to be somewhat more abundant than predicted by TNH. On the other hand, emission from Fe is well constrained by the lack of both L- and K-shell emission (dotted curve), which argues strongly against an origin in the incomplete Si-burning zone. We conclude therefore that the bright, compact knots are stellar ejecta dominated by the products of explosive O-burning that have been partially mixed with lower-Z material from layers of the star further out in radius.

Until now it has not been possible to obtain a comprehensive picture of nucleosynthesis in Cas A because of the lack of observed emission from newly synthesized iron in the ejecta. Fe

is produced in the deepest layers of the star during explosive Si burning, which, depending on the temperature of the burning front, can range from complete (resulting in nearly pure Fe) to incomplete (resulting in a spectrum of nucleosynthetic products from Si to Fe). In order to address this issue we examined two regions in Cas A that show evidence (Vink et al. 1999) for Fe K-shell emission at ∼6.7 keV and are spectrally different from each other and from the compact Si- and S-rich knots. The first, region B, is on the western edge of the remnant and appears strikingly blue in Fig. 1, while the second (C) covers a faint knot on the eastern side (red color in Fig. 1).

Previous work (e.g., Holt et al. 1994; Keohane et al. 1996; Vink et al. 1999) has noted the hardness of the X-ray emission from region B and the *Chandra* data (Fig. 3) appear to support this. The spectrum is thermal; compared to region A it is more highly absorbed and the ionization state is more advanced (i.e., note the higher intensity of the Si hydrogen-like Lymanα line at 2.0 keV compared to the helium-like lines at ∼1.85 keV). The thermodynamic state of the plasma was set to match the Fe L-shell complex at 1–1.5 keV, the Fe K-shell line at ∼6.7 keV, and the line shapes of the other bright lines. Given the state of instrumental calibration and the simplicity of our fits, the agreement between data and model is excellent. The most remarkable feature of the comparison is the inferred abundance set. The model plotted in Fig. 3 contains only the products of incomplete explosive Si-burning in the predicted ratios from TNH, plus continuum from lower Z-material. To repeat: the relative abundances of Si, S, Ar, Ca and Fe were not fitted parameters.

On the other side of the remnant is region C whose spectrum is dominated by a broad, emission feature around 1 keV. At higher energies there is a rapidly falling continuum, modest lines from Si and S, and an Fe K-shell line with an equivalent width of $W_E \sim 2000$ eV. This is a bizarre spectrum. The only abundant chemical species that can produce quasi-continuum emission around 1 keV is Fe. Our model simulations, using relative abundances from incomplete Si-burning, confirm this (dotted curve). However these fits also show that the incomplete Si-burning abundance set grossly overpredicts the Si, S, Ar, and Ca emission. A much improved fit (solid curve) results when the abundances of these species are reduced by factors of 5 or more, indicating that the composition of the knot is considerably more Fe-rich and therefore closer to that predicted for complete Si-burning. The Fe K-shell emission, as well as the shapes of the other K-shell lines, are fit quite well by this model. Differences near 1.5 keV between the data and simulations are due to the well-known deficiencies of plasma model codes for predicting the precise shape of the Fe L-shell emission (Brickhouse et al. 1995). The overall flux, which can be more accurately modeled, is in good agreement. As for both cases before, this spectrum also requires an additional source of continuum emission.

3.3. Mixing and Bulk Motion of Ejecta in Cas A

Amazingly, according to the inferred composition, the X-ray data are probing the explosive nucleosynthetic processes that occur at the highest temperatures in an supernova, i.e., the Fe- and Si-rich ejecta. Perhaps even more remarkable is the difference in the expected locations of

the products of O-burning (Si) and Si-burning (Fe). In Cas A, the most Fe-rich material lies at the outermost edge of the ejecta, while the Si-rich ejecta is generally closer to the center. This is best seen on the eastern side of the remnant, where fingers of Fe-rich material (red color in Fig. 1) clearly precede the Si-rich knots (whitish color in Fig. 1). (The lack of Si beyond the Fe emission, as well as a lack of Fe inside the Si-emission, argues against projection effects.) The conclusion is obvious: the ejecta in Cas A have undergone a spatial inversion or overturning of the explosive O- and Si-burning products. It is also clear, however, that this process did not lead to a homogenization of this portion of the ejecta, since we see individual knots produced by the different burning processes.

Previous evidence (Fesen & Gunderson 1996) for mixing of inner and outer layers of Cas A has come from optical spectroscopy of knots in the "jet" toward the northeast, which can be seen in the *Chandra* image as a few faint linear wisps of X-ray emission. The presence in a dozen or so optical knots of explosive O-burning products (O, S, and Ar) that also contained H and N from the star's outer layers was taken as a sign that mixing had occurred between the O-burning zone and the hydrostatic layers of the star. We appear to require this type of mixing as well, since all three of our extracted spectra require additional low Z-material to explain the observed level of continuum emission (note that some fraction of the continuum may be coming from other processes, see §3.4). However, our results also require the bulk motion of significant fractions of the Si-burning zone out past the O-burning zone during the explosion that formed Cas A. This inversion of the nucleosynthetic products points to a considerably more extensive, energetic, and violent process of large-scale mixing than previously observed, although mixing of this type has been proposed to explain the light curve and the early appearance of X-ray and γ-rays from SN1987A (see Woosley 1988 and references therein).

The theoretical basis for large scale mixing and bulk motions of ejecta has also been established recently. Modelers now recognize the importance of neutrino-driven convection for initiating core-collapse SN explosions (Herant et al. 1994; Burrows, Hayes, & Fryxell 1995). Multidimensional radiation/hydrodynamics simulations of this process show that it results in a massively aspherical explosion that includes "crooked fingers" of ejecta blown out at high speeds. Homogenization of the material is not expected because any single parcel of core matter undergoes neutrino-driven convection for only one or two cycles of rising and falling. At later times, the radioactive decay energy of ^{56}Ni ($\sim 10^{17}$ ergs gm^{-1}), which is comparable to the kinetic energy density in the "Fe"-rich ejecta ($\sim 2 \times 10^{16}$ ergs gm^{-1}) (Woosley 1988), may play a role. We note that the bright compact knots in the remnant are nearly all Si-rich (the bright whitish and greenish structures in Fig. 1), while the knots of Fe-rich ejecta (red features) tend to be more diffuse and extended. This is suggestive of an additional heating source in the Fe-rich knots which could be the radioactive decay energy. However, until theoretical studies tell us how the formation, evolution, and motion of ejecta knots depends on their position in the star, it will be difficult to quantify the amount of additional heating required to explain the more diffuse nature of the Fe-rich knots.

3.4. Featureless Continuum Emission

Spectra of enriched stellar ejecta alone do not provide a complete picture of Cas A. Some regions within the remnant show no evidence for thermal emission; their spectra are devoid of line emission. Region D contains one such filament that we selected based on its curious purple color suggesting an intrinsic spectrum weak in Si K-shell emission. Indeed the extracted spectrum is nearly featureless; the equivalent widths of the Ne, Mg, Si, S, Ar, Ca, and Fe K-shell lines are all less than 200 eV. It is well described by an absorbed power-law model with a photon index of $\alpha \sim 2.6$, but could be fit equally well by an absorbed thermal continuum with $kT \sim 2.5$ keV. For the filament to be purely thermal it would need to have very low abundances of the species from Ne through Fe. One possibility is that we are seeing a portion of the blast wave in the ISM in which the metals have been depleted onto dust grains (e.g., Vancura et al. 1994). This is unlikely, since some chemical species, Ne and Ar especially, are not expected to be depleted. Furthermore, the *Chandra* spectrum of the blast wave (the faint outer shelf of emission) does clearly show significant Si and S emission lines. Another possibility is that this filament is thermal continuum from low Z material, similar to what we argue above underlies the thermal, metal-rich spectra of the several ejecta knots that we studied.

It is more likely that this filament is emitting X-ray synchrotron radiation from high energy electrons that have been accelerated to TeV energies in the SN shock like in SN1006 (Koyama et al. 1995) and G347.3−0.5 (Koyama et al. 1997; Slane et al. 1999). The photon index is comparable to the values measured from these other SNRs (∼1.9 and ∼2.5, respectively) in which nonthermal synchrotron radiation dominates the X-ray emission in the 2-10 keV band. Furthermore, Allen et al. (1997) inferred the presence of nonthermal power-law emission from Cas A underlying the predominantly thermal emission in the band below 16 keV. Their power-law index, $\alpha = 1.8^{+0.5}_{-0.6}$, is broadly consistent with what we find here, especially given the simplicity of their model for the thermal emission and our calibration uncertainties. This raises the possibility that some or even all of the continuum emission we argued for above is nonthermal, rather than thermal.

4. SUMMARY

We find that the Cas A SNR contains compact, high surface brightness knots enriched in Si and S that are consistent with the nucleosynthetic products of explosive O-burning. Moreover the observed equivalent widths of the line features in the knots require the presence of continuum emission from material with low atomic number ($Z < 8$) indicating that the core and mantle of the star were mixed during the SN explosion, as also found by others. Elsewhere in the remnant we find more diffuse, lower surface brightness features with abundances that are consistent with explosive Si-burning. These features contain a considerable amount of Fe, which in some cases dominates the X-ray emission, and this is what differentiates them from the O-burning products.

Remarkably these Fe-rich features lie at the outer edge of the bright regions that mark the distribution of the SN ejecta. Since explosive Si-burning occurs at greater depths in the progenitor star than O-burning does, these results require that a spatial inversion of a significant portion of the star's core has occurred. This was likely the result of neutrino-driven convection during the initiation of the SN explosion. The radioactive decay energy of ^{56}Ni may explain the more diffuse nature of the Fe-rich ejecta knots. Finally we have discovered faint, sharply defined filaments with nearly featureless spectra that are likely to be emitting nonthermal radiation and may be indicating the sites of cosmic ray shock acceleration in Cas A. This brief report barely touches on the wealth of information and new discoveries that will be forthcoming as we study the *Chandra* data on this and other SNRs.

This work would not have been possible without the dedication, sacrifice, and hard work of the literally thousands of scientists, engineers, technicians, programmers, analysts, and managers who worked on the *Chandra* X-ray Observatory during the long course of its development. Special thanks are offered to them. Helpful discussions with Anne Decourchelle and Thomas Douvion on the scientific content of the article are gratefully acknowledged. We appreciate Monique Arnaud's support and hospitality during the course of this project. This work was partially supported by NASA Grant NAG5-6420.

REFERENCES

Allen, G. E., et al. 1997, ApJ, 487, L97

Brickhouse, N., et al. 1995, Legacy, 6, 4

Burrows, A., Hayes, J. & Fryxell, B. 1995, ApJ, 450, 830

Fesen, R. A., Becker, R. H. & Blair, W. P. 1987, ApJ, 313, 378

Fesen, R. A. & Gunderson, K. S. 1996, ApJ, 470, 967

Garmire, G. P. 1997, BAAS, mtg # 190, #34.04

Herant, M., Benz, W., Hix, W. R., Fryer, C. L., & Colgate, S. A. 1994, ApJ, 435, 339

Holt, S. S., Gotthelf, E. V., Tsunemi, H. & Negoro, H. 1994, PASJ 46, L151

Hughes, J. P. & Singh, K. P. 1994, ApJ, 422, 126

Keohane, J. W., Rudnick, L. & Anderson, M. C. 1996, ApJ, 466, 309

Koyama, K., Petre, R., Gotthelf, E. V., Hwang, U., Matsura, M., Ozaki, M., & Holt, S. S. 1995, Nature, 378, 255

Koyama, K., Kinugasa, K., Matsuzaki, K., Nishiuchi, M., Sugizaki, M., Torii, K., Yamauchi, S., & Aschenbach, B. 1997, PASJ, 49, L7.

Murray, S. S., Fabbiano, G., Fabian, A. C., Epstein, A. & Giacconi, R. 1979, ApJ, 234, 69

Reed, J. E., Hester, J. J., Fabian, A. C. & Winkler, P. F. 1995, ApJ, 440, 706

Ryle, M. & Smith, F.G. 1948, Nature, 162, 462

Slane, P., Gaensler, B. M., Dame, T. M., Hughes, J. P., Plucinsky, P. P., & Green, A. 1999, ApJ, in press (1 Nov)

Thielemann, F.-K., Nomoto, K., & Hashimoto, M. 1996, ApJ, 460, 408 (TNH)

Vancura, O., Raymond, J. C., Dwek, E., Blair, W. P., Long, K. S., & Foster, S. 1994, ApJ, 431, 188

Vink, J., Maccarone, M. C., Kaastra, J. S., Mineo, T., Bleeker, J. A. M., Preite-Martinez, A. & Bloemen, H. 1999, A&A, 344, 289

Weisskopf, M. C., O'Dell, S. L., Van Speybroeck, L. P. 1996, Proc. SPIE 2805, Multilayer and Grazing Incidence X-Ray/EUV Optics III, 2.

Woosley, S. E. 1988, ApJ, 330, 218

Woosley, S. E. & Weaver, T. A. 1995, ApJS, 101, 181

Fig. 1.— *Chandra* X-ray image of Cas A, encoding information on the intrinsic X-ray spectrum. The figure was constructed from images in three different energy bands: 0.6–1.65 keV (red), 1.65–2.25 keV (green), and 2.25–7.50 keV (blue). The images contained a total of 4.1×10^5, 2.9×10^5, and 1.9×10^5 X-ray events with peak number of events (in any single $1''$ square pixel) of 59, 89, and 47, respectively. The separate images were square-root scaled from 0 to 80% of their individual peak values after being smoothed to a signal-to-noise ratio per pixel of 7 by a Gaussian function whose width depended on the local image intensity. The main effect of the smoothing process was to make the faint outer regions of the remnant visible; the bright, high spatial frequency parts of the images were unaffected.

Fig. 2.— Broadband *Chandra* X-ray image of Cas A. The spectral extraction regions in our study are indicated.

Fig. 3.— Energy spectra from several regions in Cas A as indicated in figure 2. The horizontal error bars show the widths of the energy bins and the vertical ones indicate the statistical error on the measured event rate; systematic errors are not included. Superposed on the data points are smooth curves of simulated *Chandra* ACIS-S spectra. The simulations for regions A, B and C are of a shock-heated plasma with nonequilibrium ionization fractions absorbed by line-of-sight interstellar material. The dotted curves in regions A and C, and the solid curve for region B, assume abundances corresponding to explosive incomplete Si-burning. A considerably better match for region A uses O-burning abundances (solid curve). The solid curve for region C is more Fe-rich, the Si, S, Ar, and Ca abundances are reduced by factors of 5 or more from their values in incomplete Si-burning. The solid curves for regions A, B, and C have temperatures of 2.5 keV, 2.5 keV, and 2.8 keV, ionization timescales of 2.5×10^{10} cm^{-3} s^{-1}, 7.9×10^{10} cm^{-3} s^{-1}, and 7.9×10^{10} cm^{-3} s^{-1}, and column densities of 0.9×10^{22} atoms cm^{-2}, 2.3×10^{22} atoms cm^{-2}, and 1.5×10^{22} atoms cm^{-2} respectively. All the models for regions A, B and C also include significant amounts of continuum emission from material with lower atomic number. The solid curve for region D is an absorbed power-law model with a photon index of 2.6 and column density 1.3×10^{22} atoms cm^{-2}.

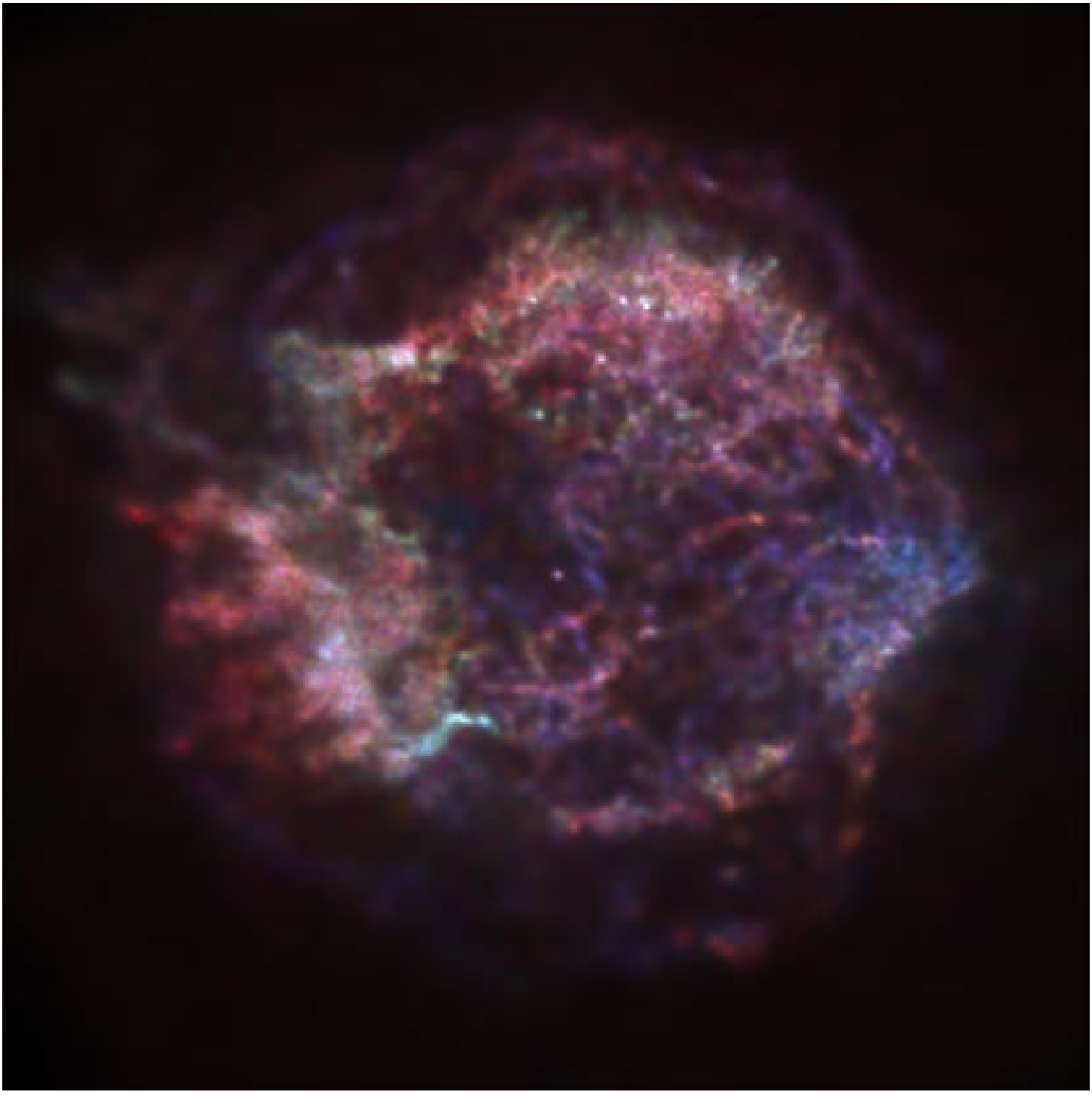

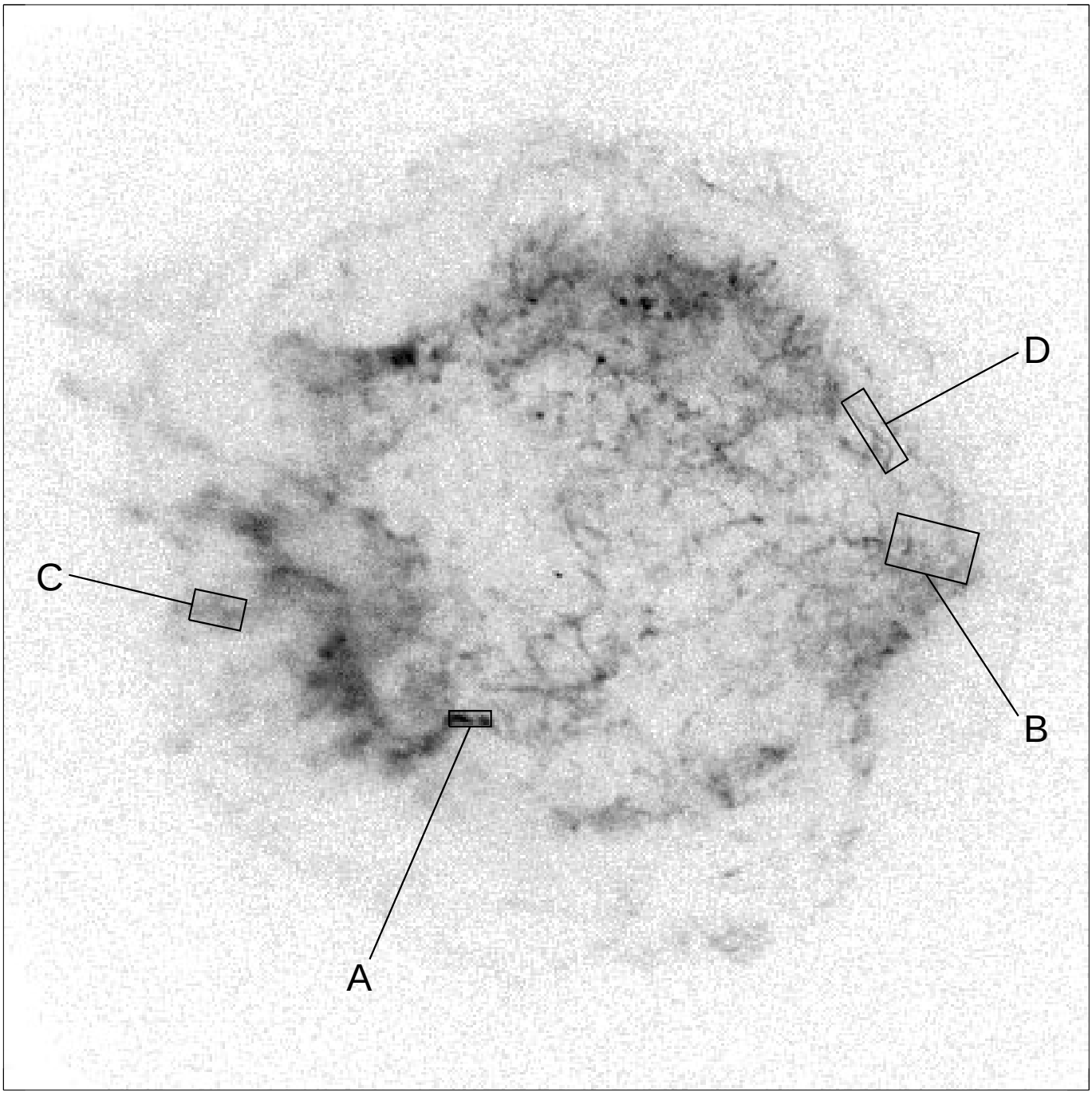
Cas A 0.6-7.5 keV band
Chandra X-ray Observatory
D
C
B
A

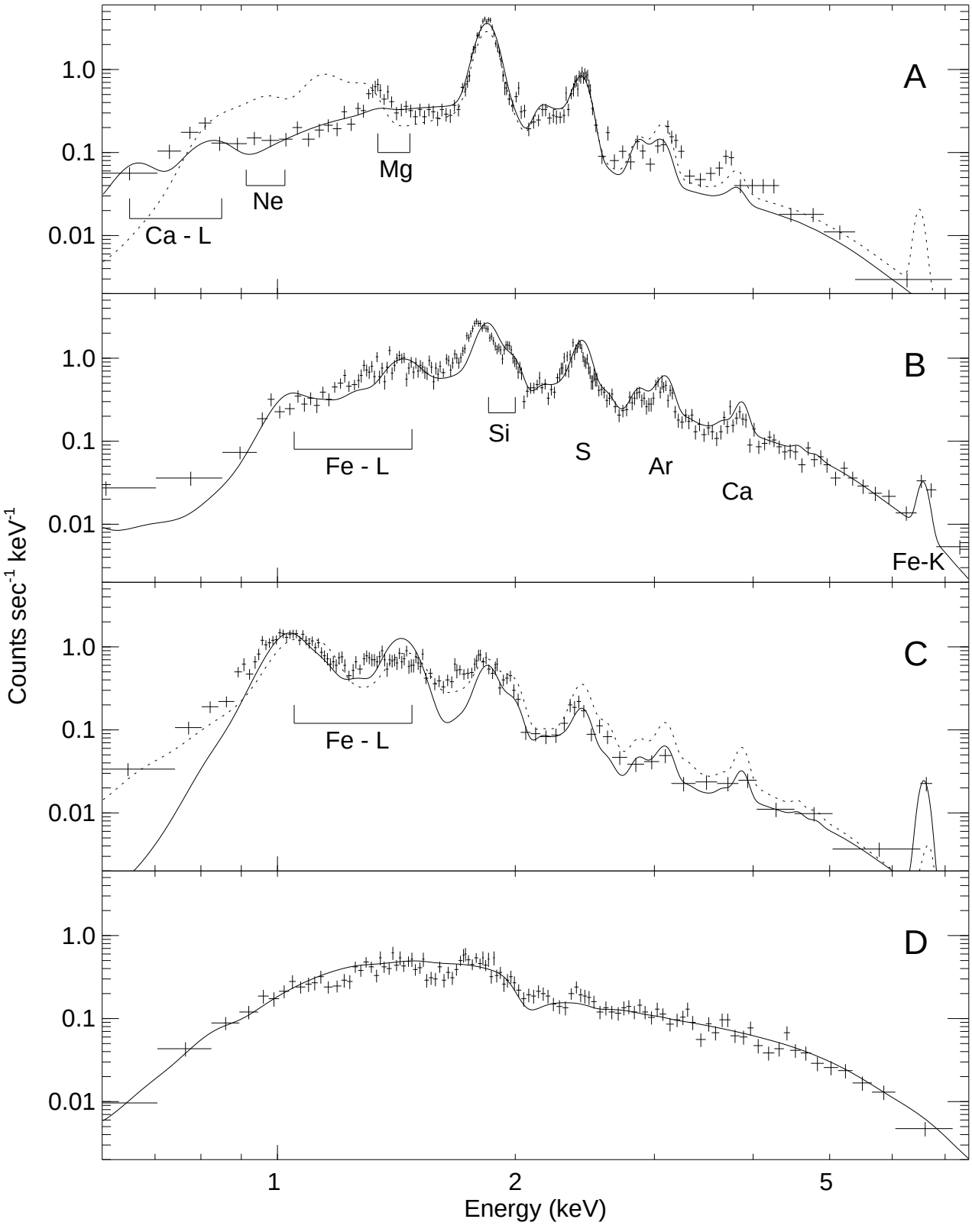
A
B
C
D
Ca - L
Ne
Mg
Fe - L
Si
S
Ar
Ca
Fe-K
Fe - L
1.0
0.1
0.01
1
2
5
Energy (keV)
Counts sec-1 keV-1

Cas A 0.6-7.5 keV band Chandra X-ray Observatory

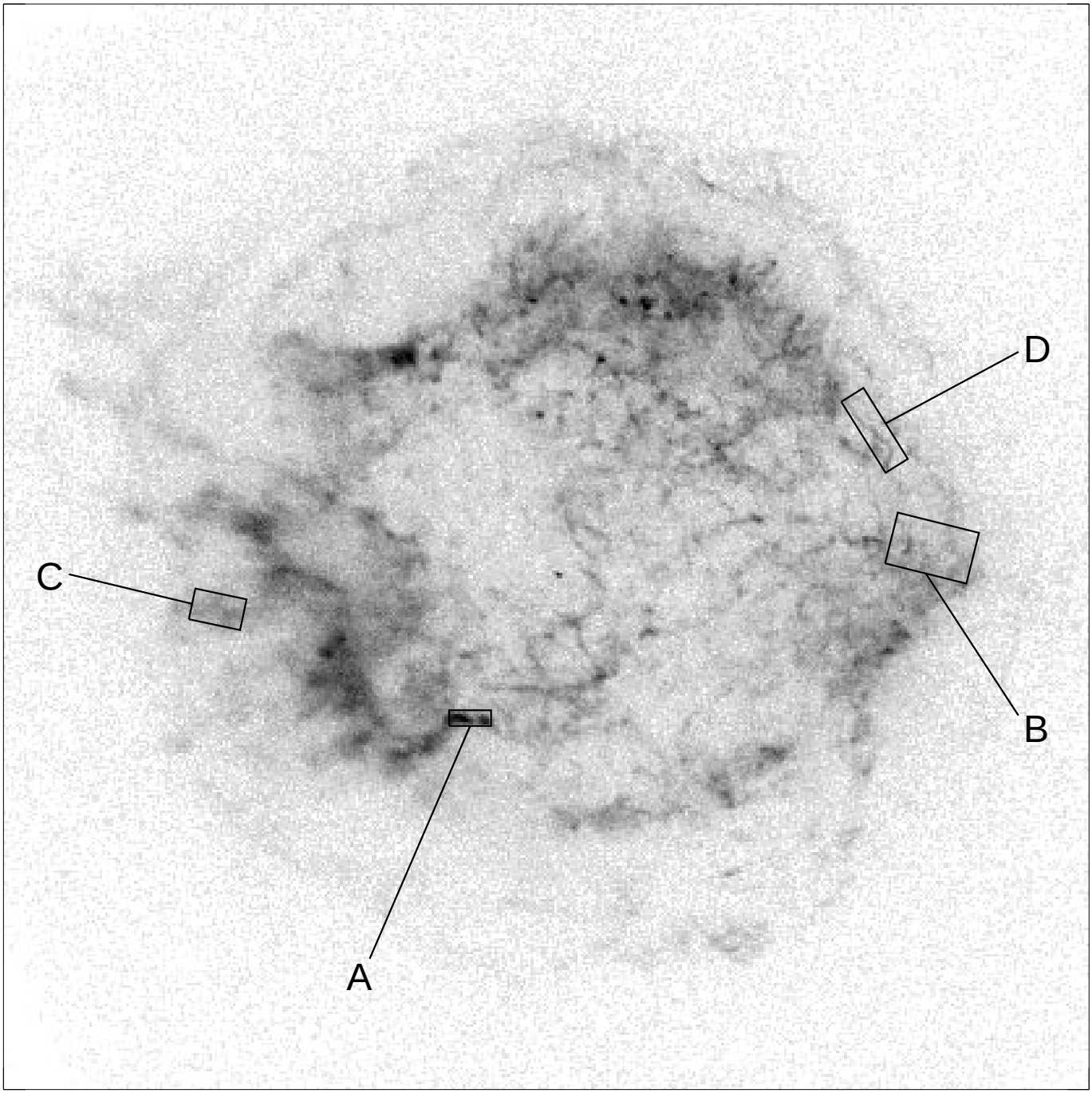

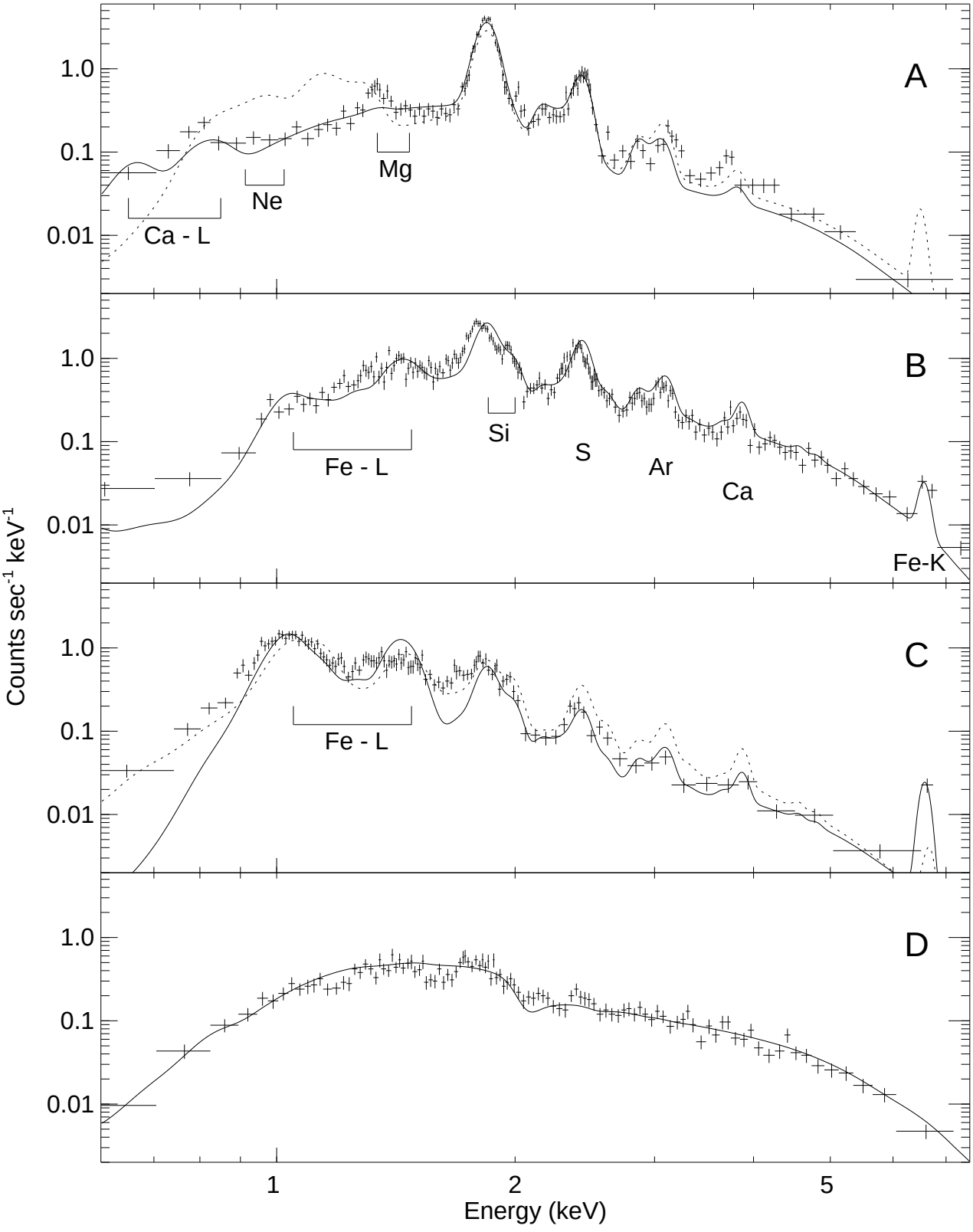
A
B
C
D
Ca - L
Ne
Mg
Fe - L
Si
S
Ar
Ca
Fe-K
Fe - L
1.0
0.1
0.01
1
2
5
Energy (keV)
Counts sec-1 keV-1